Supporting Information

High-stability NIR-II Fluorescence Polymer Synthesized by Atom Transfer Radical Polymerization for High-Resolution NIR-II Imaging Application

*Kun He [a†], Shangyu Chen [a†], Wenjuan Xu [a], Xiaoyan Tai [a], Yan Chen [a], Pengfei Sun [*a], Quli Fan [*a] and Wei Huang [b]*

[a] State Key Laboratory of Organic Electronics and Information Displays & Institute of Advanced Materials (IAM), Nanjing University of Posts & Telecommunications, 9 Wenyuan Road, Nanjing 210023, China.

[b] Frontiers Science Center for Flexible Electronics (FSCFE), MIIT Key Laboratory of Flexible Electronics (KLoFE), Northwestern Polytechnical University, Xi'an 710072, China.

Experimental section

Materials.

4,8-Bis(5-bromo-4-(2-octyldodecyl)thiophen-2-yl)-1H,3H-benzo[1,2-c:4,5-c']bis([1,2,5]thiadiazole) (BBT), 6,7-Bis(4-(hexyloxy)phenyl)-4,9-di(thiophen-2-yl)-[1,2,5]thiadiazolo[3,4-g]quinoxaline (TTQ), 4,6-bis(5-bromo-2-thienyl)thieno[3,4-c][1,2,5]thiadiazole (TTDT), 9,9'-spirobi[fluoren]-2-yltributylstannane (SF) and 9,9-dioctyl-9H-fluorene (F) were purchased from Suna Tech Inc(Suzhou Industrial Park, Jiangsu, China). Other catalysts were purchased from commercial sources (such as Aldrich, J&K Scientific Ltd., and Sigma-Aldrich). Unless indicated, all synthetic procedures were performed in an anhydrous and oxygen free environment. These regents were used without further purification, except toluene, which was dried and distilled with N_2 before use. Dulbecco's Modified Eagle's Medium (DMEM, Gibco, U.S.) was obtained from Gene Tech Co. (Shanghai, China).

Characterizations.

Nuclear magnetic resonance (NMR) spectra were recorded on a Bruker Ultra Shield Plus 400 MHz spectrometer (^{1}H, 400 MHz, Bruker Electronics, Billerica, MA, USA) by using tetramethylsilane as the internal standard. The UV-vis-NIR spectra were

recorded on a Shimadzu UV-3600 UV-vis-NIR spectrophotometer (Tokyo, Japan). All UV tests were conducted at room temperature. The morphology of nanoparticles was determined by transmission electron microscope (HT7700, TEM) with an acceleration voltage of 100 KV. Dynamic light scattering (DLS) analysis was conducted on a commercial laser light scattering spectrometer (ALV-7004, ALV) equipped with a multi-τ digital time correlator and a He–Ne laser (at λ = 632.8 nm). A CONTIN analysis was used to extract the average hydrodynamic diameter (D_h) data. All test samples were prepared and made optically clean by filtration through 0.45 mm Millipore filters before measurement and each sample was tested three times. The scattering angle was 90° and all measurements were carried out at room temperature. The NIR-II fluorescence spectrum of three small molecules and nanoparticles (NPs) were measured using a NIR-II spectroscopy (Fluorolog 3) with InGaAs NIR detector under an 808 nm diode laser (RMPC lasers) excitation. The *in vitro* and *in vivo* NIR-II FI experiments were conducted on an NIR-II imaging system (Wuhan Grand-imaging Technology Co., Ltd) with 1064 filters under 808 nm laser irradiation. A 640 × 512 pixel two-dimensional InGaAs array from Princeton Instruments in NIR-II fluorescence windows was equipped in this NIR-II FI system. The NIR-II fluorescence image-guided tumor surgery were tested using fluorescence image assisted theragnostic-Light (FIAT-L, Nawoo Vision Co., Ltd).

Synthesis of the BBT-SF

The mixture of BBT (108 mg, 0.1 mmol), 9,9'-spirobi[fluoren]-2-yltributylstannane (181 mg, 0.3 mmol), P(o-Tol)$_3$ (14 mg) and $Pd_2(dba)_3$ (4 mg) in anhydrous toluene (8 mL) were treated by freeze-thaw cycles for three times, and then heated to 100 °C under argon atmosphere. After cooling, the obtained crude product was evaporated to remove toluene and purified by using column chromatography to acquire the product BBT-SF (74 mg, 47.8%).

Synthesis of the TTQ-SF

The mixture of TTQ (86 mg, 0.1 mmol), 9,9'-spirobi[fluoren]-2-yltributylstannane (181 mg, 0.3 mmol), P(o-Tol)$_3$ (14 mg) and $Pd_2(dba)_3$ (4 mg) in anhydrous toluene (8 mL) were treated by freeze-thaw cycles for three times, and then heated to 100 °C under argon atmosphere. After cooling, the obtained crude product was evaporated to remove toluene and purified by using column chromatography to acquire the product BBT-SF (104 mg, 78.8%).

Synthesis of the TTDT-SF

The mixture of TTDT (46.4 mg, 0.1 mmol), 9,9'-spirobi[fluoren]-2-yltributylstannane (181 mg, 0.3 mmol), P(o-Tol)$_3$ (14 mg) and $Pd_2(dba)_3$ (4 mg) in chlorobenzene (8 mL) were treated by freeze-thaw cycles for three times, and then heated to 135 °C under argon atmosphere. After cooling, the obtained crude product was evaporated to remove toluene and purified by using column chromatography to acquire the product TTDT-SF (65 mg, 69.5%).

Quantum yield test.

The fluorescence quantum yields (QY) of three small molecule were measured by using the method described in a previous study[1]. The QY were determined according to the reference fluorophore IR1061, which has a QY value of 1.7 ± 0.5% in dichloromethane (DCM). The parameter n is the refractive index of solvent. Five different concentrations around or less than an OD of 0.1 (approximately 0.1, 0.08, 0.06, 0.04, and 0.02) were measured, and all samples were analyzed at 25 °C. After comparing the slopes of the integrated fluorescence, which was plotted against the absorbance for both the reference and samples, the QY was calculated using the following equation:

$$QY_{(sample)} = QY_{(ref)} \times \frac{slope_{(sample)}}{slope_{(ref)}} \times \frac{n^2_{(sample)}}{n^2_{(ref)}}$$

The 4T1 tumor models.

All experiments using animals were performed according to the specifications of The National Regulation of China for Care and Use of Laboratory Animals, and the protocol was approved by the Jiangsu Administration of Experimental Animals. 4T1 tumor-bearing mice (age 5-6 weeks) were obtained from the Jiangsu Kaiji Biotechnology Co., LTD. 4T1 tumors were planted by hypodermic injection of suspension of 4T1 cells into the right armpit of mice. The tumor volume was calculated as the following equation:

$$V=0.5\ LW^2$$

The parameter L and W are the longitudinal and transverse diameters of the tumor, respectively.

The orthotopic brain tumor models.

Five or six-week-old Balb/c athymic nude mice were chose for the construction of brain tumor model. Fix the head of the anesthetized mice with a brain locator, drill a hole in the anterior lobe of the mice's brain, and then inject 10 μL U87 MG cells suspension in PBS. Tumors can be formed after about two weeks of breeding.

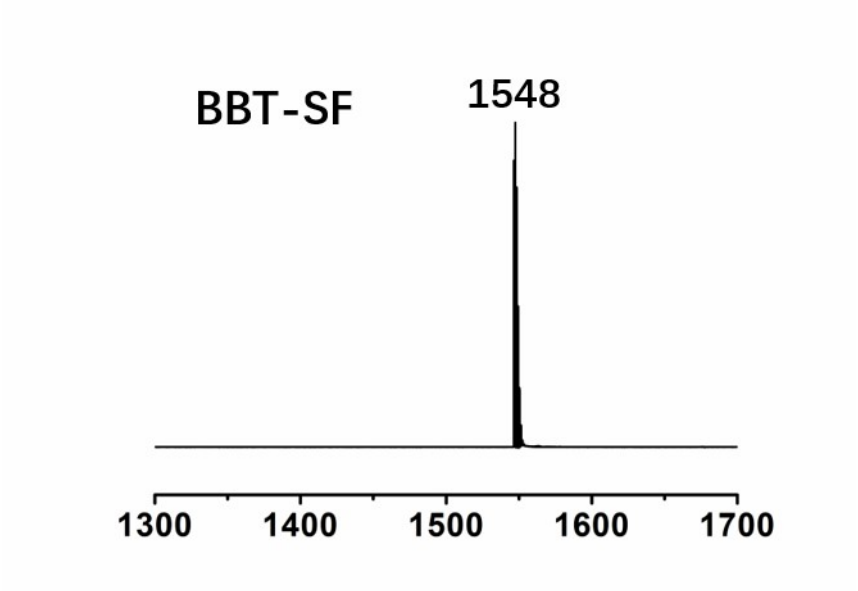

Figure S1. MALDI-TOF mass spectrometry of BBT-SF.

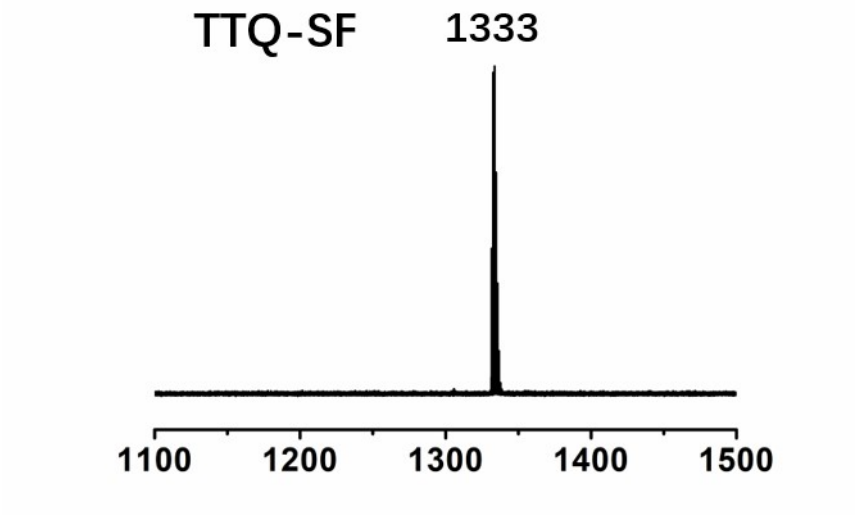

Figure S2. MALDI-TOF mass spectrometry of TTQ-SF.

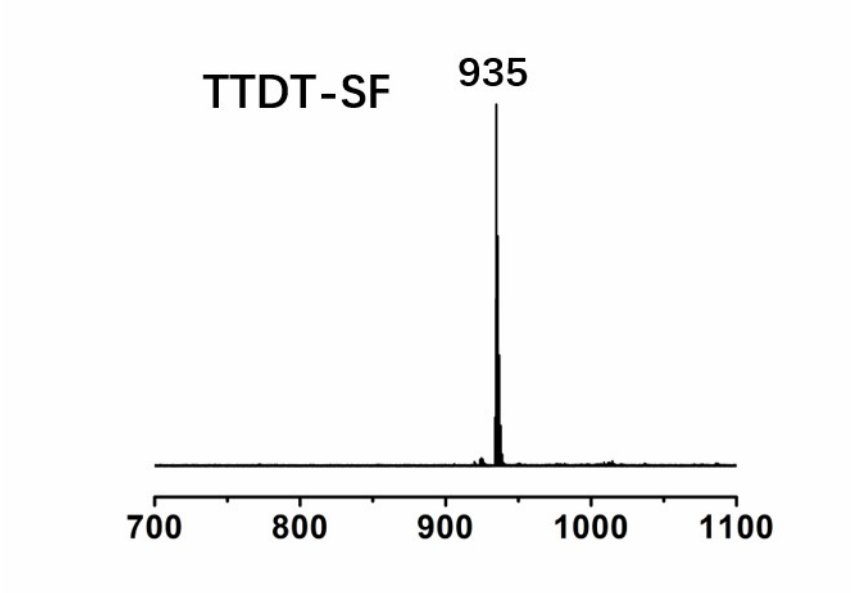

Figure S3. MALDI-TOF mass spectrometry of TTDT-SF.

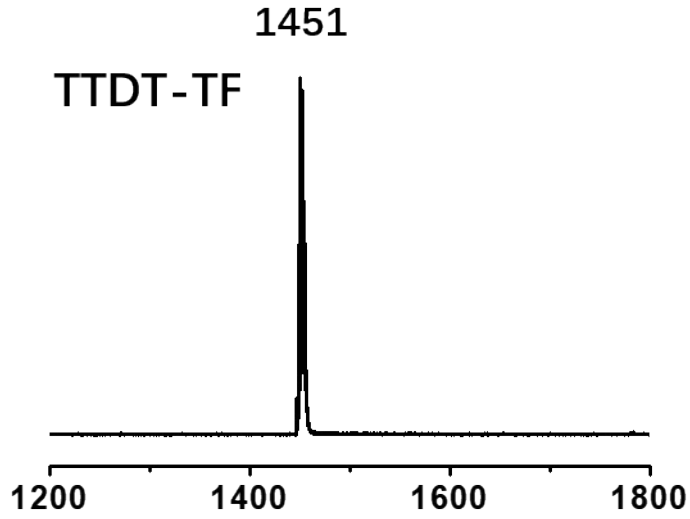

Figure S4. MALDI-TOF mass spectrometry of TTDT-TF.

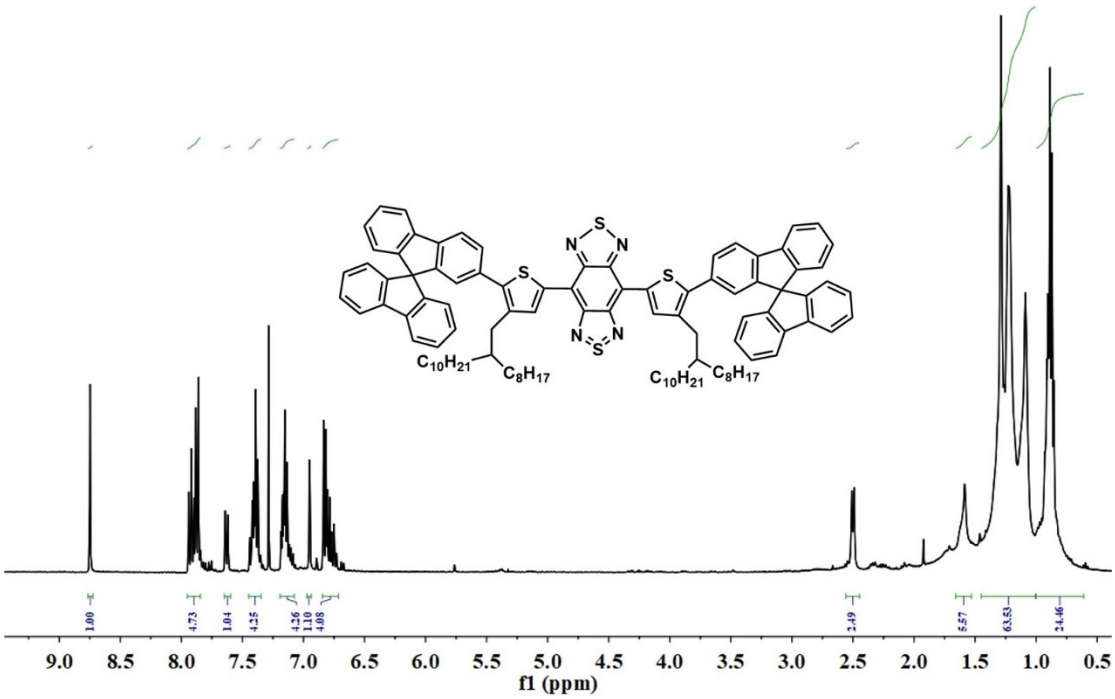

Figure S5. ^{1}H NMR spectrum of BBT-SF in $CDCl_3$.

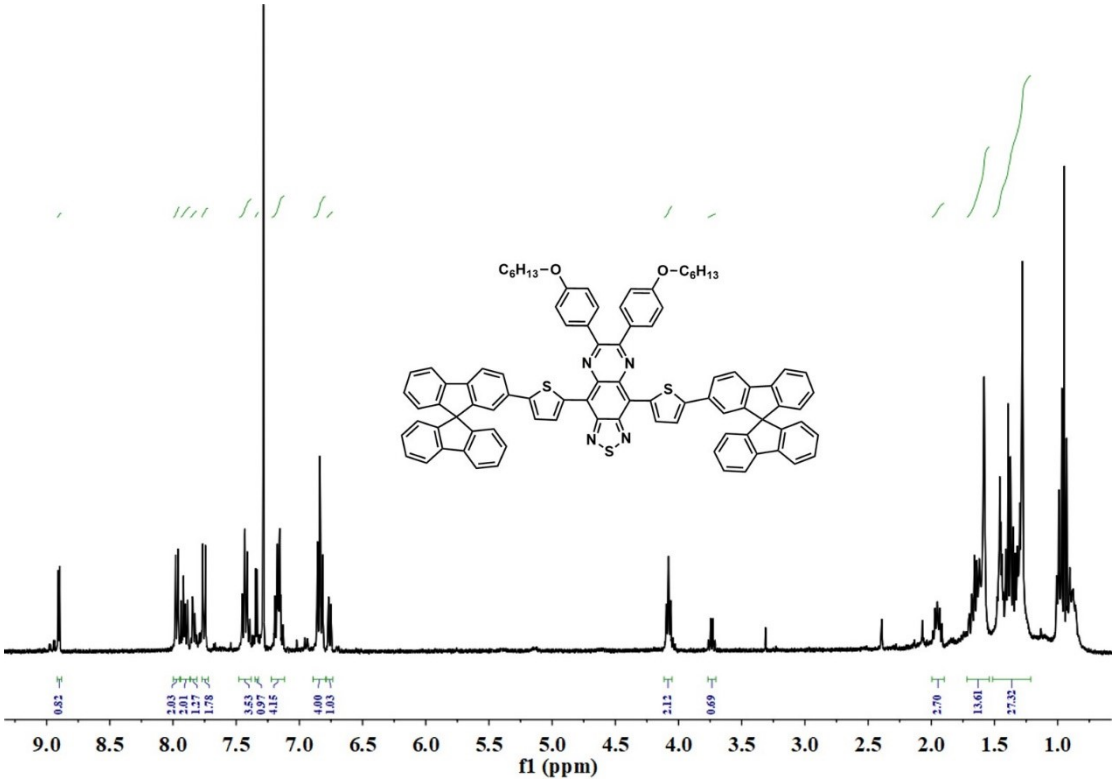

Figure S6. ^{1}H NMR spectrum of TTQ-SF in $CDCl_3$.

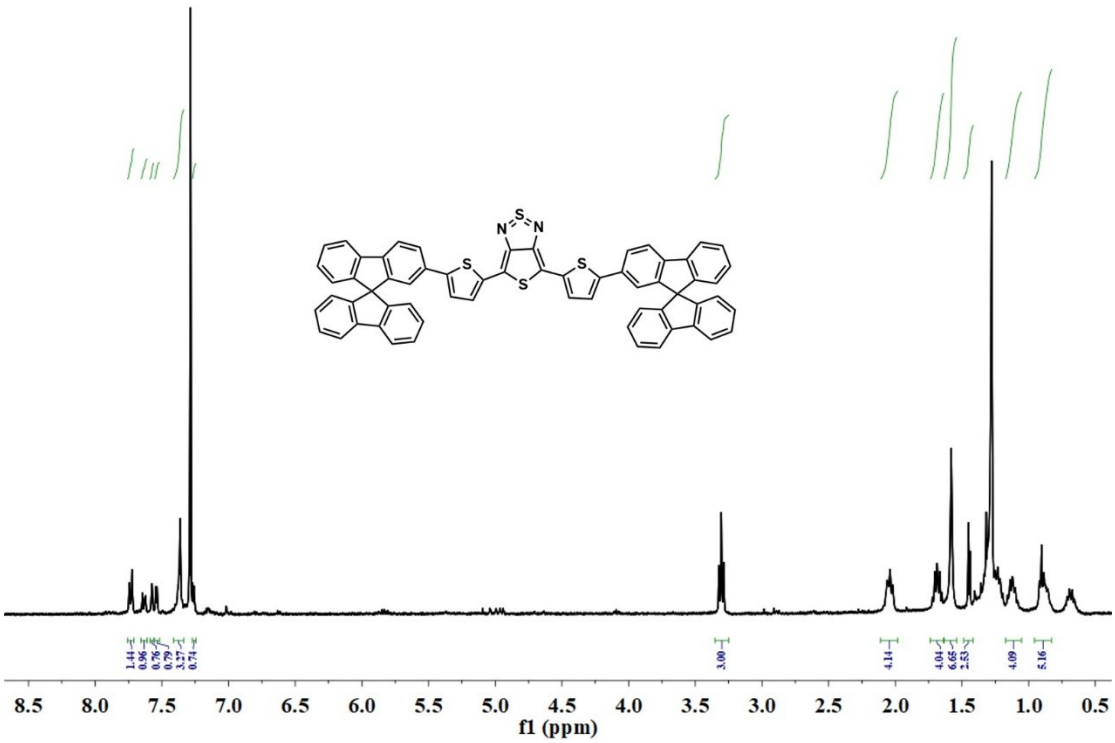

Figure S7. ^{1}H NMR spectrum of TTDT-SF in $CDCl_3$.

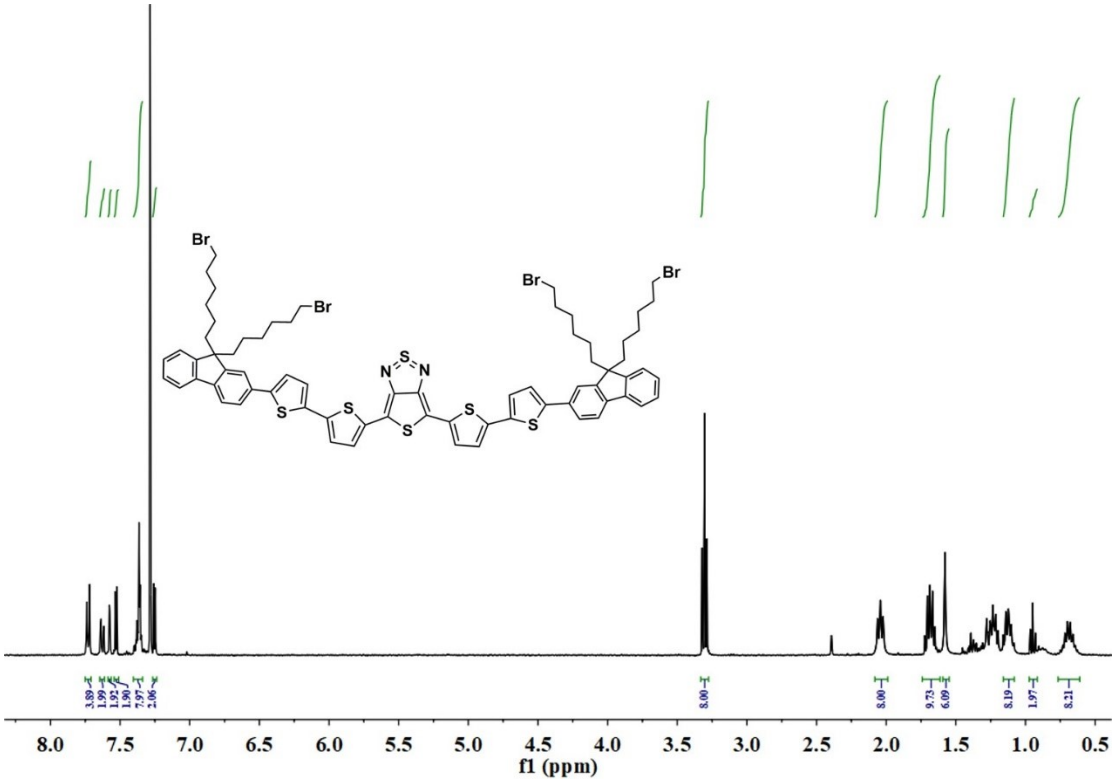

Figure S8. ^{1}H NMR spectrum of TTDT-TF in $CDCl_3$.

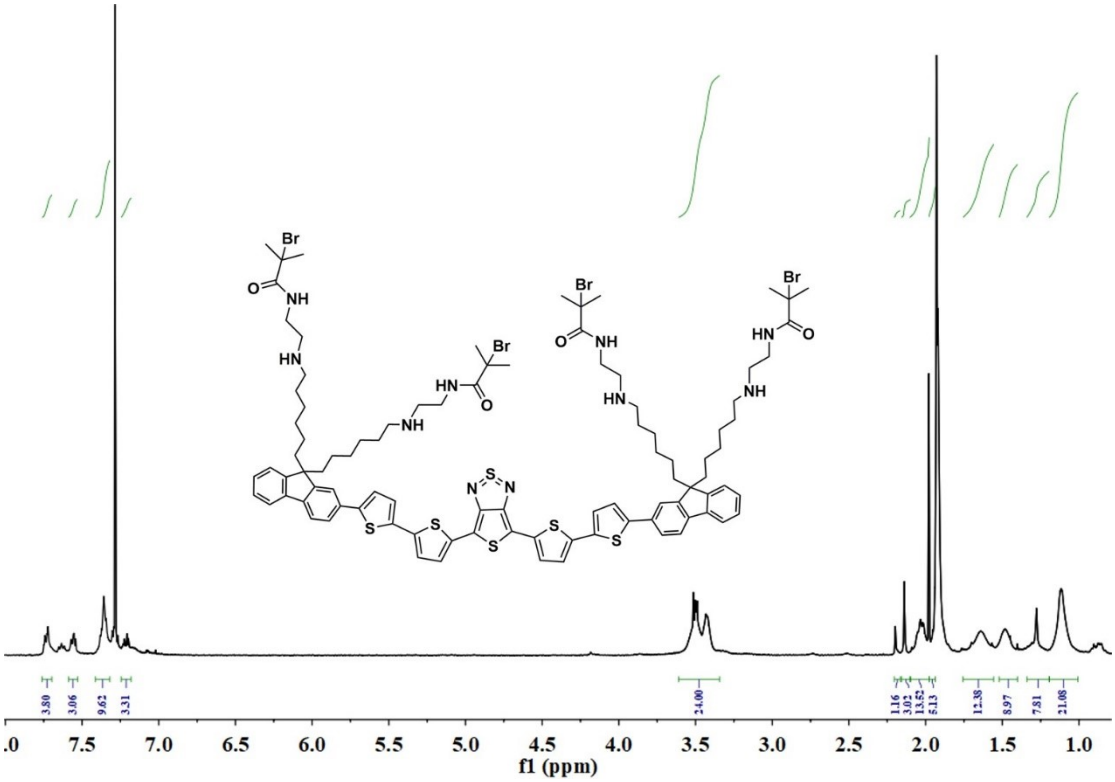

Figure S9. ^{1}H NMR spectrum of TTDT-TF-Br in $CDCl_3$.

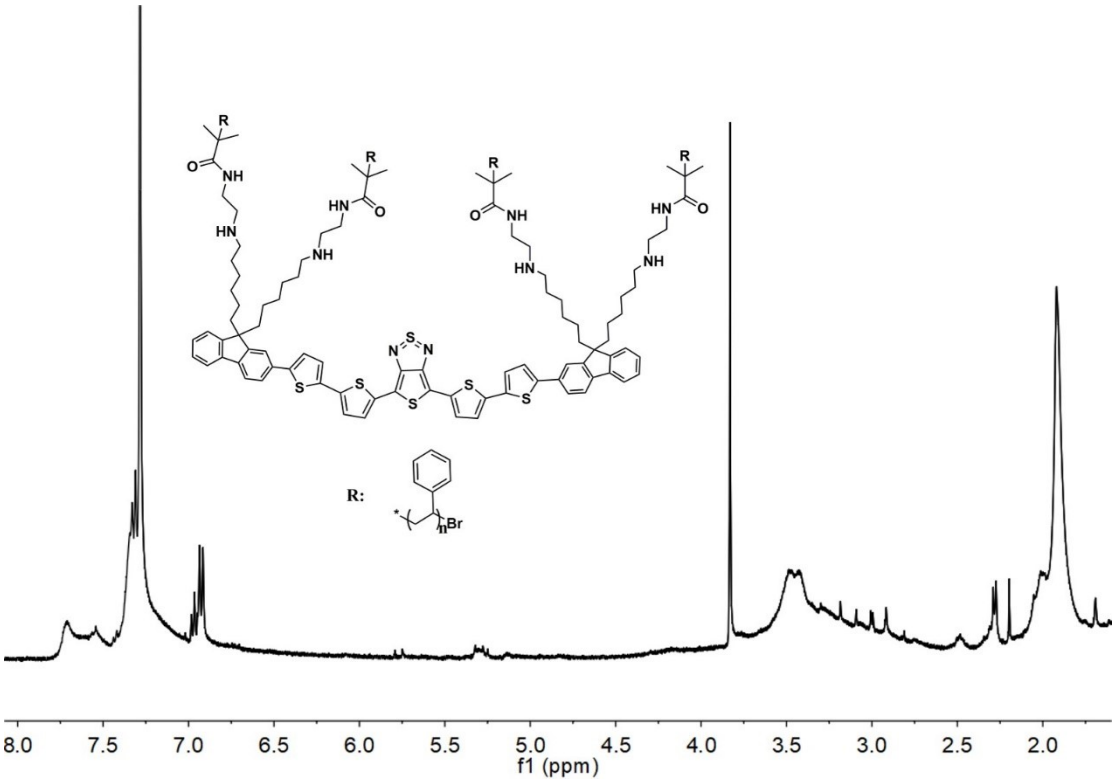

Figure S10. ^{1}H NMR spectrum of TTDT-TF-PS in $CDCl_3$.

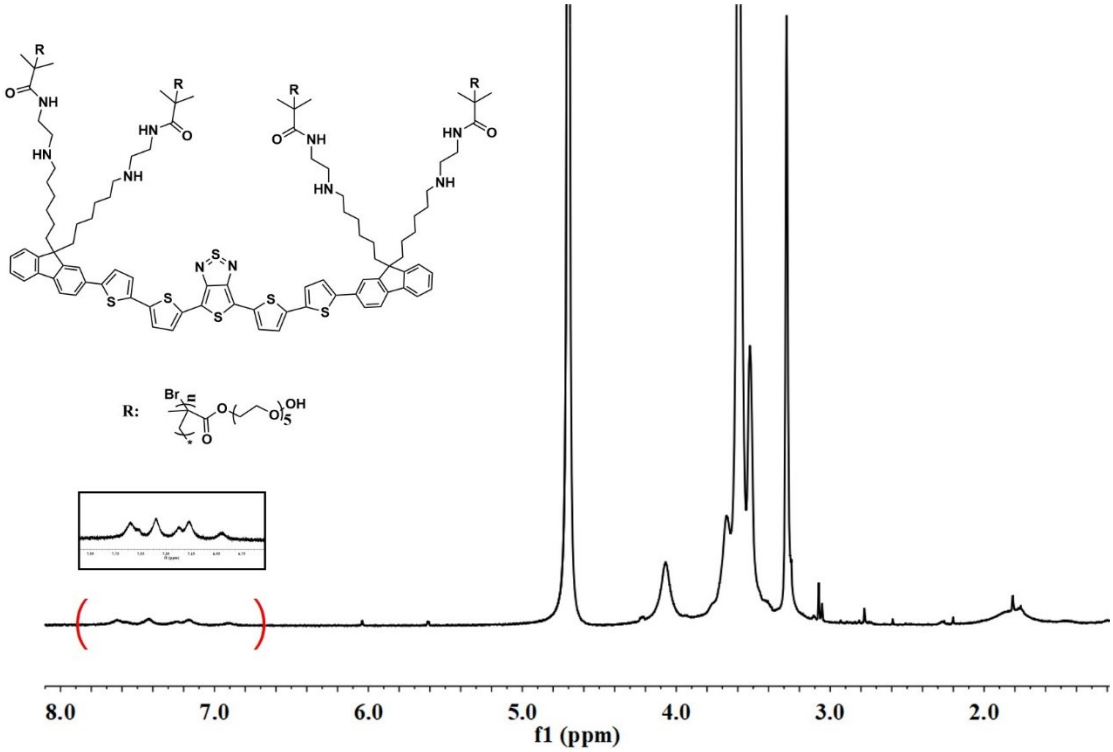

Figure S11. ^{1}H NMR spectrum of TTDT-TF-POEGMA in D_2O.

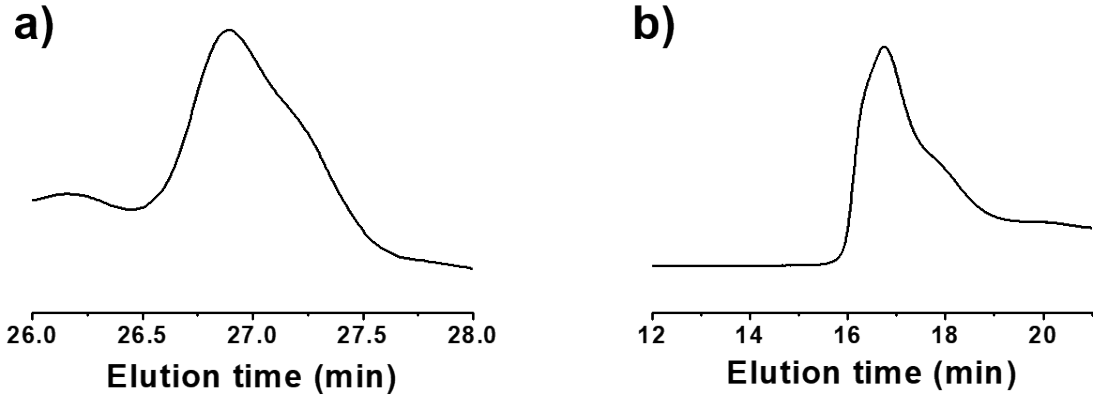

Figure S12. The GPC curve of (a) TTDT-TF-PS and (b) TTDT-TF-POEGMA.

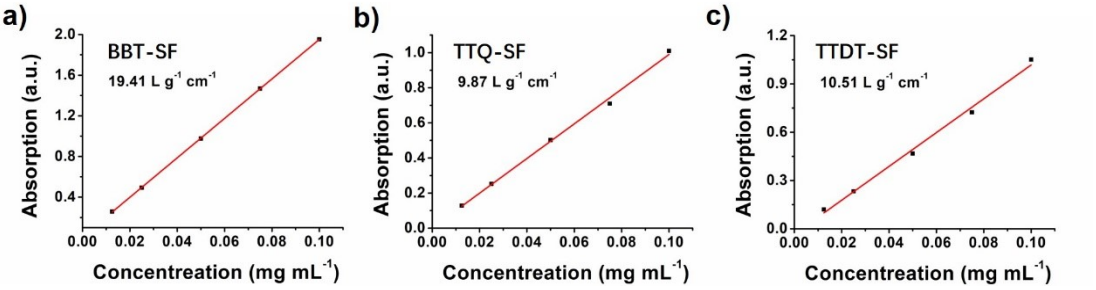

Figure S13. The extinction coefficients of (a) BBT-SF, (b) TTQ-SF, and (c) TTDT-SF in the dilute THF solution, respectively.

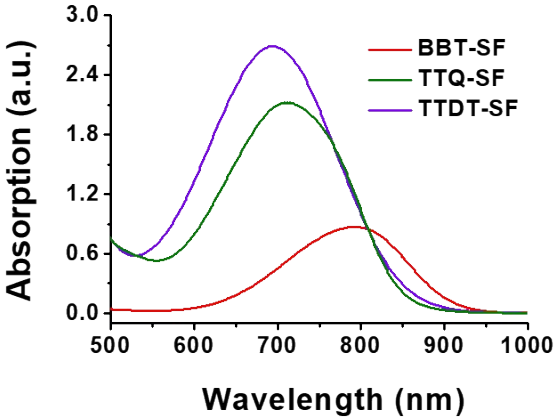

Figure S14. The absorption spectrum of BBT-SF, TTQ-SF, and TTDT-SF in THF, respectively.

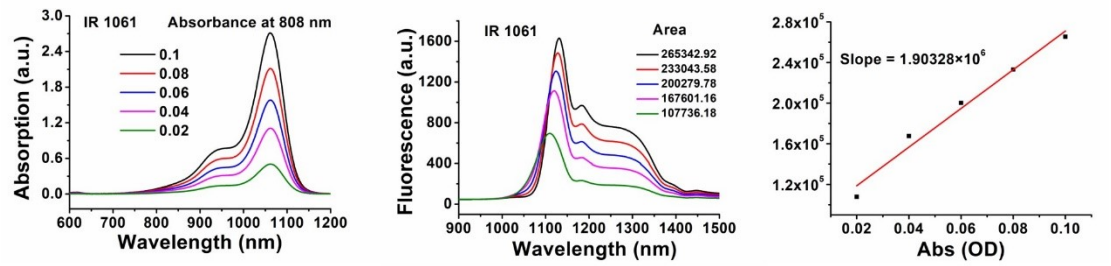

Figure S15 Absorption and fluorescence emission spectra and relatively quantified analysis of IR 1061 in DCM.

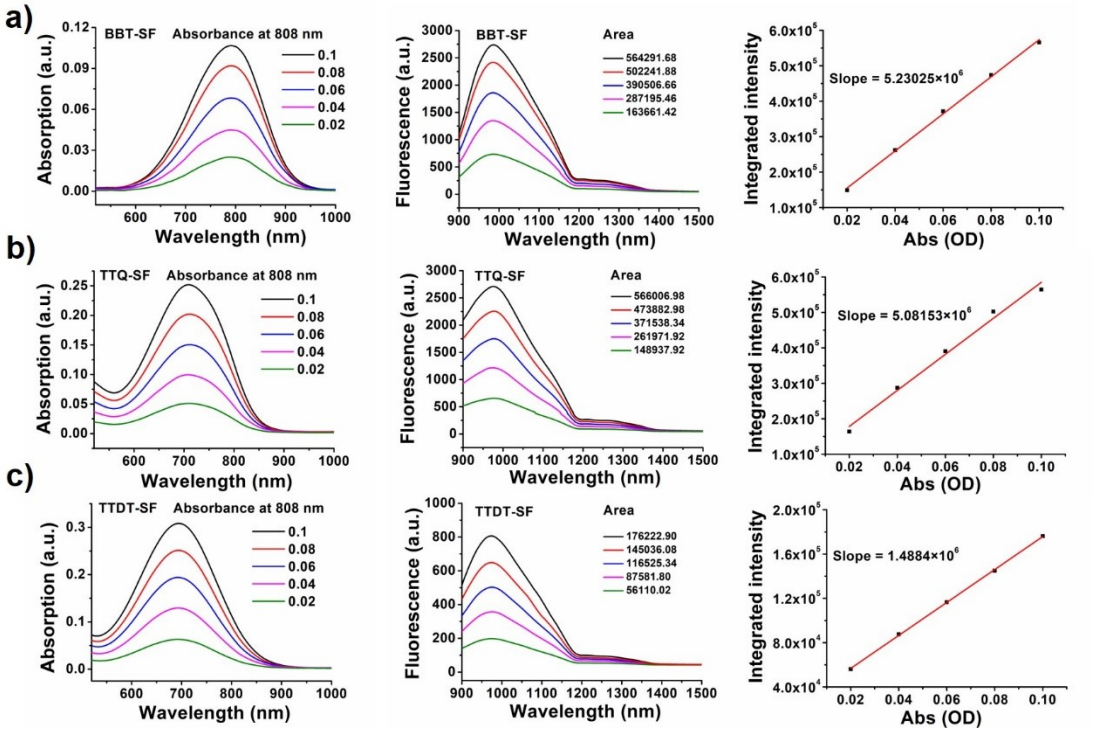

Figure S16. Quantum yield measurement of BBT-SF, TTQ-SF, and TTDT-SF with IR 1061 as the reference sample. Absorption and fluorescence emission spectra and relatively quantified analysis of (a) BBT-SF, (b) TTQ-SF, and (c) TTDT-SF in THF.

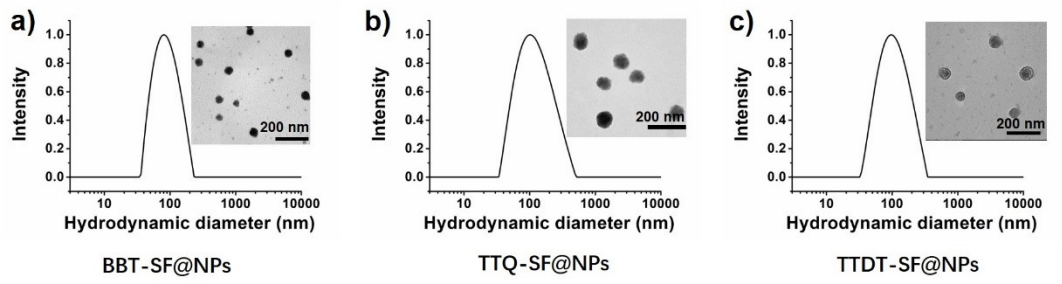

Figure S17. The size distribution of (a) BBT-SF@NPs, (b) TTQ-SF@NPs, and (c) TTDT-SF@NPs. The TEM image of BBT-SF@NPs, TTQ-SF@NPs, and TTDT-SF@NPs were shown in the inset image.

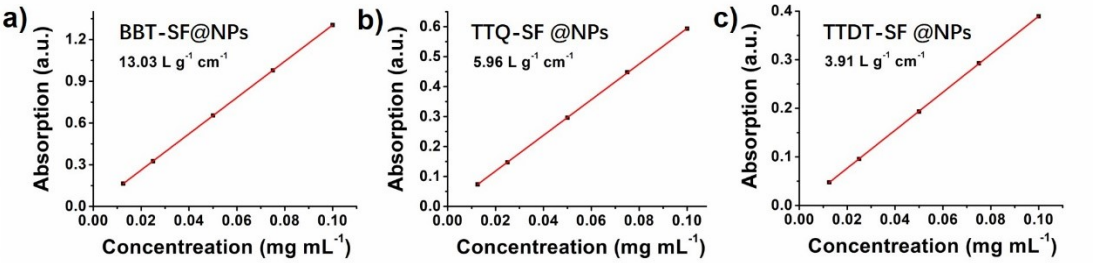

Figure S18. The extinction coefficients of (a)BBT-SF@NPs, (b)TTQ-SF@NPs, and (c)TTDT-SF@NPs in the water, respectively.

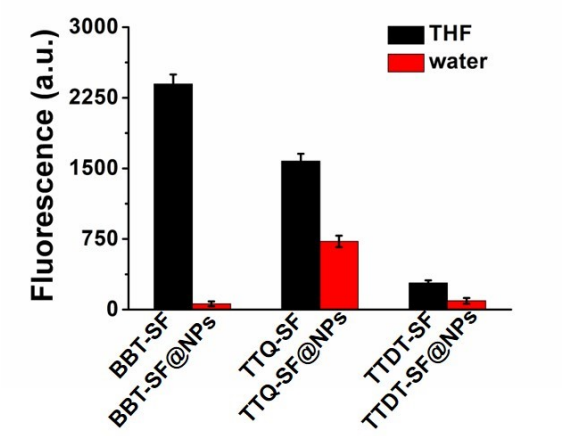

Figure S19. The fluorescence quenching of BBT-SF@NPs, TTQ-SF@NPs, and TTDT-SF@NPs.

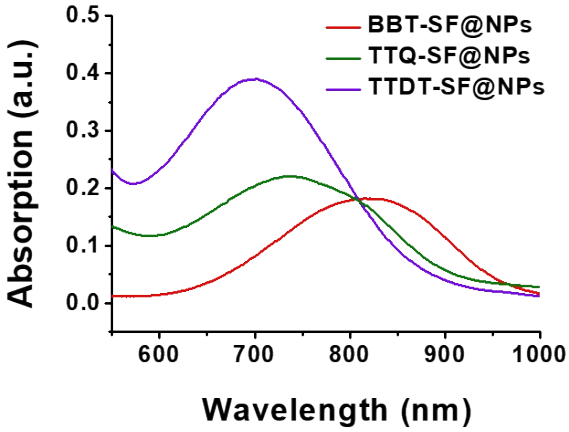

Figure S20. The absorption spectrum of BBT-SF@NPs, TTQ-SF@NPs, and TTDT-SF@NPs in water, respectively.

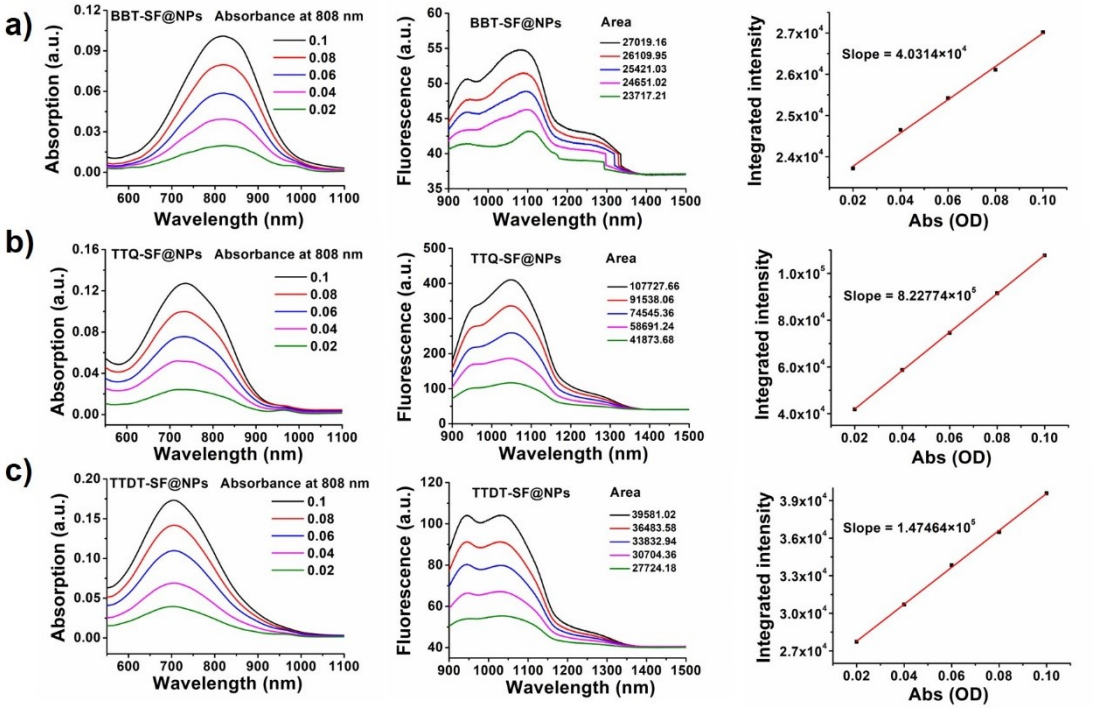

Figure S21. Quantum yield measurement of BBT-SF@NPs, TTQ-SF@NPs, and TTDT-SF@NPs with IR 1061 as the reference sample. Absorption and fluorescence emission spectra and relatively quantified analysis of (a) BBT-SF@NPs, (b) TTQ-SF@NPs, and (c) TTDT-SF@NPs in aqueous solution.

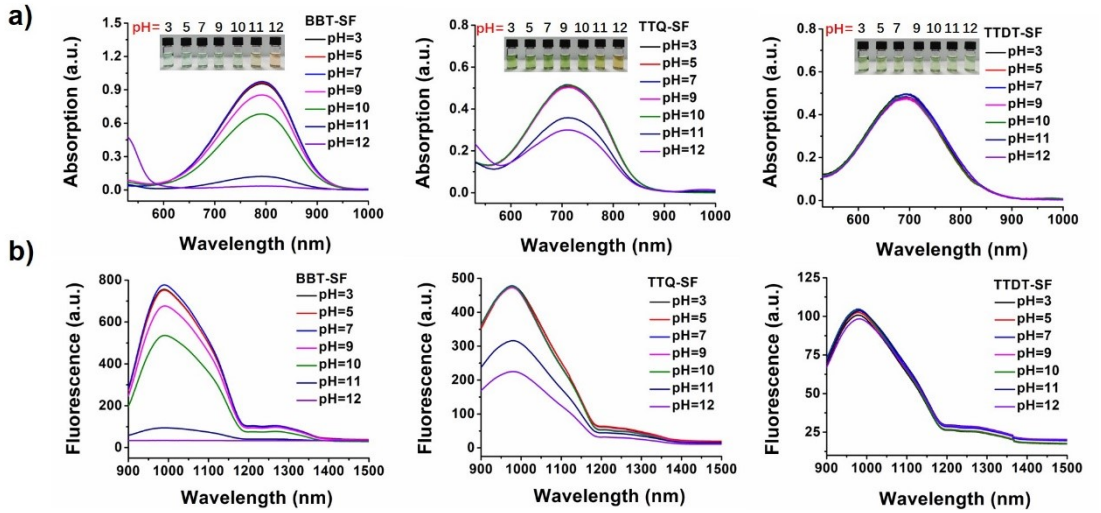

Figure S22. (a) The absorption spectra, corresponding photographs (inset) and (b) fluorescence spectra of BBT-SF, TTQ-SF, and TTDT-SF under different pH environment, respectively.

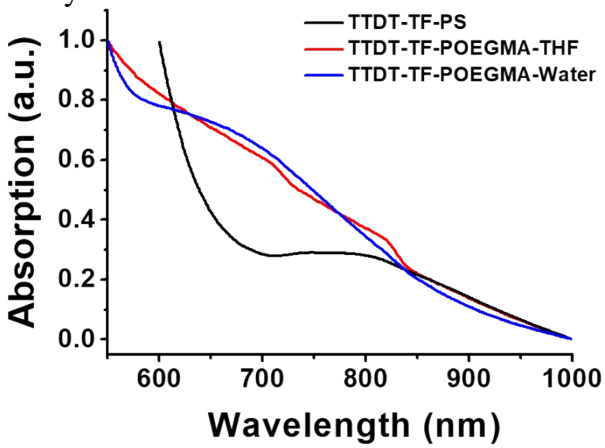

Figure S23. The absorption spectra of TTDT-TF-PS and TTDT-TF-POEGMA in THF and TTDT-TF-POEGMA in aqueous solution.

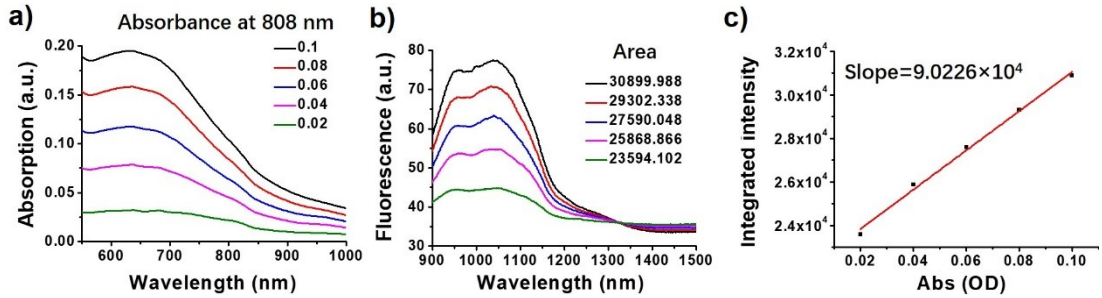

Figure S24. Quantum yield measurement of TTDT-TF-POEGMA with IR 1061 as the reference sample. (a) Absorption and (b) fluorescence emission spectra and (c) relatively quantified analysis of TTDT-TF-POEGMA in water.

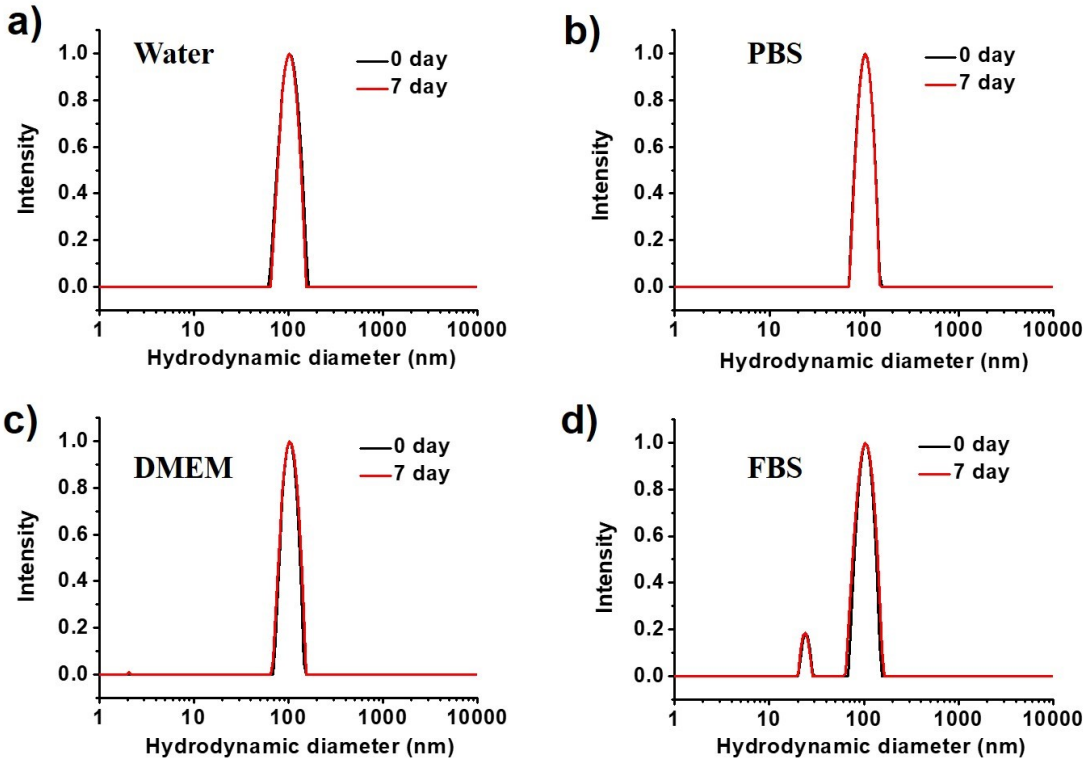

Figure S25. The size stability of TTDT-TF-POEGMA in (a) water, (b) PBS, (c) DMEM, and (d) FBS.

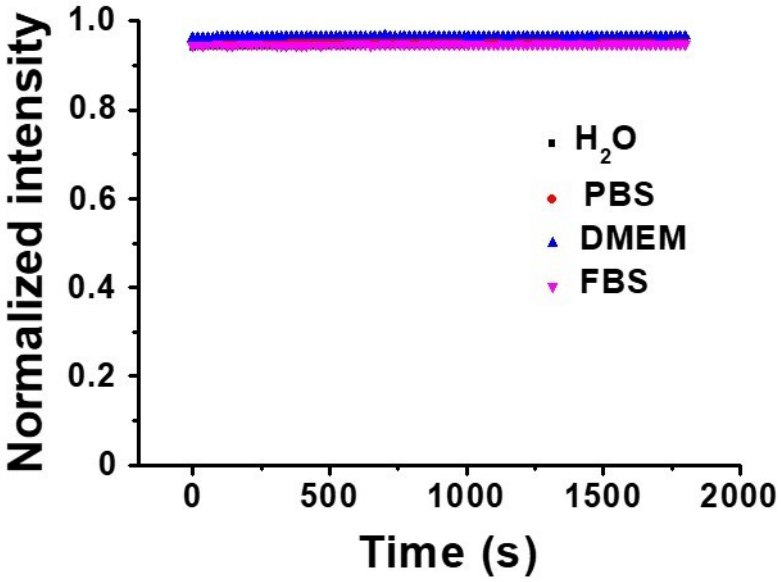

Figure S26. The photostability of TTDT-TF-POEGMA in water, PBS, DMEM, and FBS.

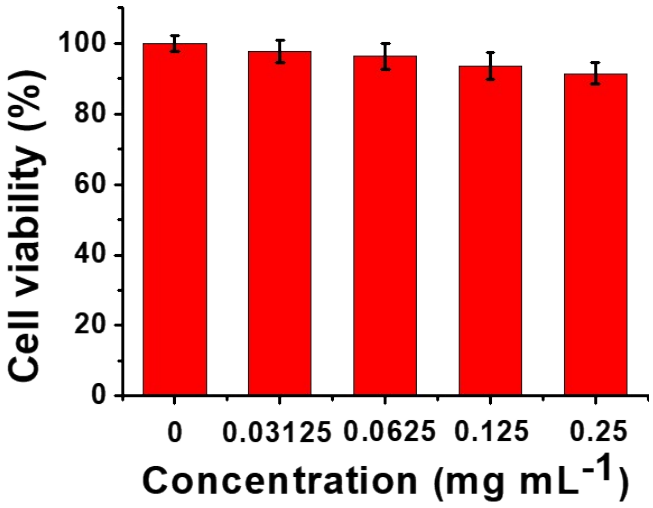

Figure S27. Cell viability of NIH 3T3 cell after incubation with TTDT-TF-POEGMA at various concentrations for 48 h.

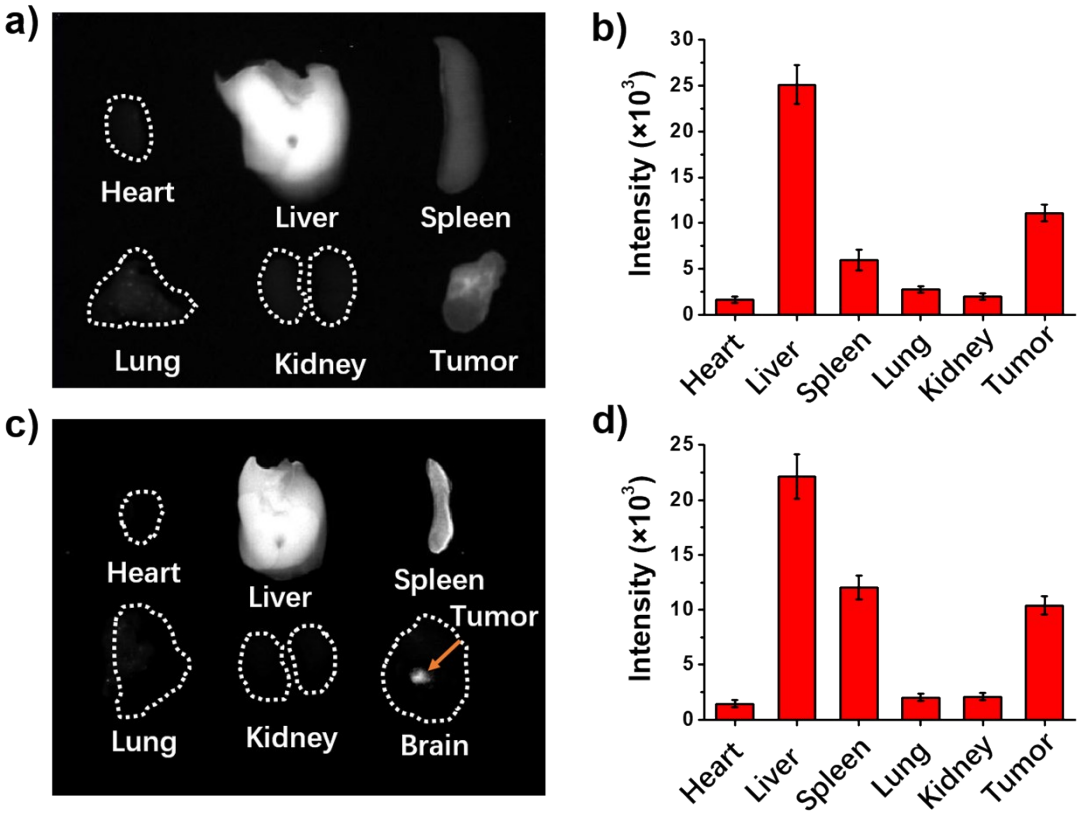

Figure S28. (a) Ex vivo NIR-II fluorescence images of major organs (heart, liver, spleen, lung, and kidney) and tumor after 36 h of intravenous injection. (b) Quantitative NIR-II fluorescence intensity of major organs and tumor. (c) In vitro NIR-II fluorescence images of major organs (heart, liver, spleen, lung, kidney, and brain) after 36 h of intravenous injection. (d) Quantitative NIR-II fluorescence intensity of major organs and tumor.

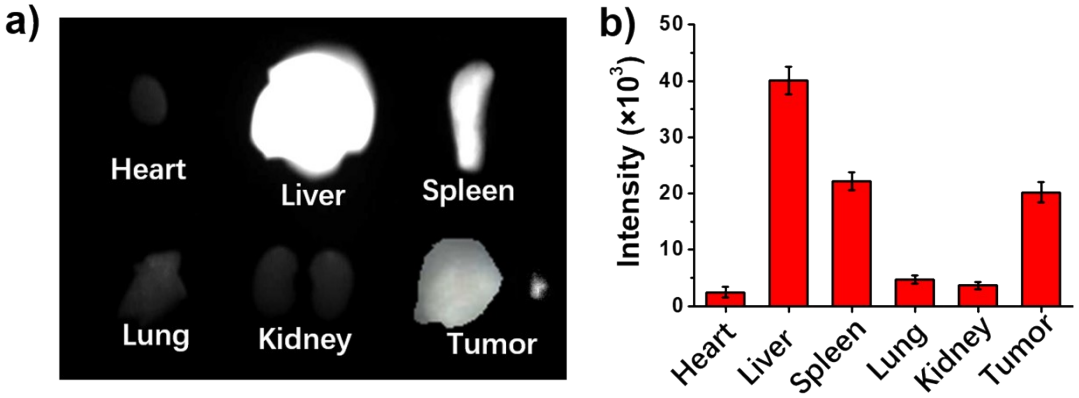

Figure S29. (a) Ex vivo NIR-II fluorescence images of major organs (heart, liver, spleen, lung, and kidney) and tumor after 36 h of intravenous injection. (b) Quantitative NIR-II fluorescence intensity of major organs and tumor.

Reference

1. M. Casalboni, F. De Matteis, P. Prosposito, *Chem. Phy. Lett.*, 2003, **373**, 372-378.